

Supporting information

Data-Driven Optimization for Controllable Multi-Scale Aperture Fabrication of Nanopipettes

Runan Guo^a, Zhi Chen^a, Xue Han^{a,e}, Rongke Sun^a, Hui Lu^{a,e}, Yanqing Ma^{a,b,c,d*}

and Lei Ma^{a,b,c*}

^a Tianjin International Center for Nanoparticles and Nanosystems, Tianjin University, 300072, P. R. China. Tianjin University, 300072, P. R. China

^b Tianjin Key Laboratory for Low-dimensional Electronic Materials and Advanced Instrumentation, Tianjin University, 300072, P.R. China.

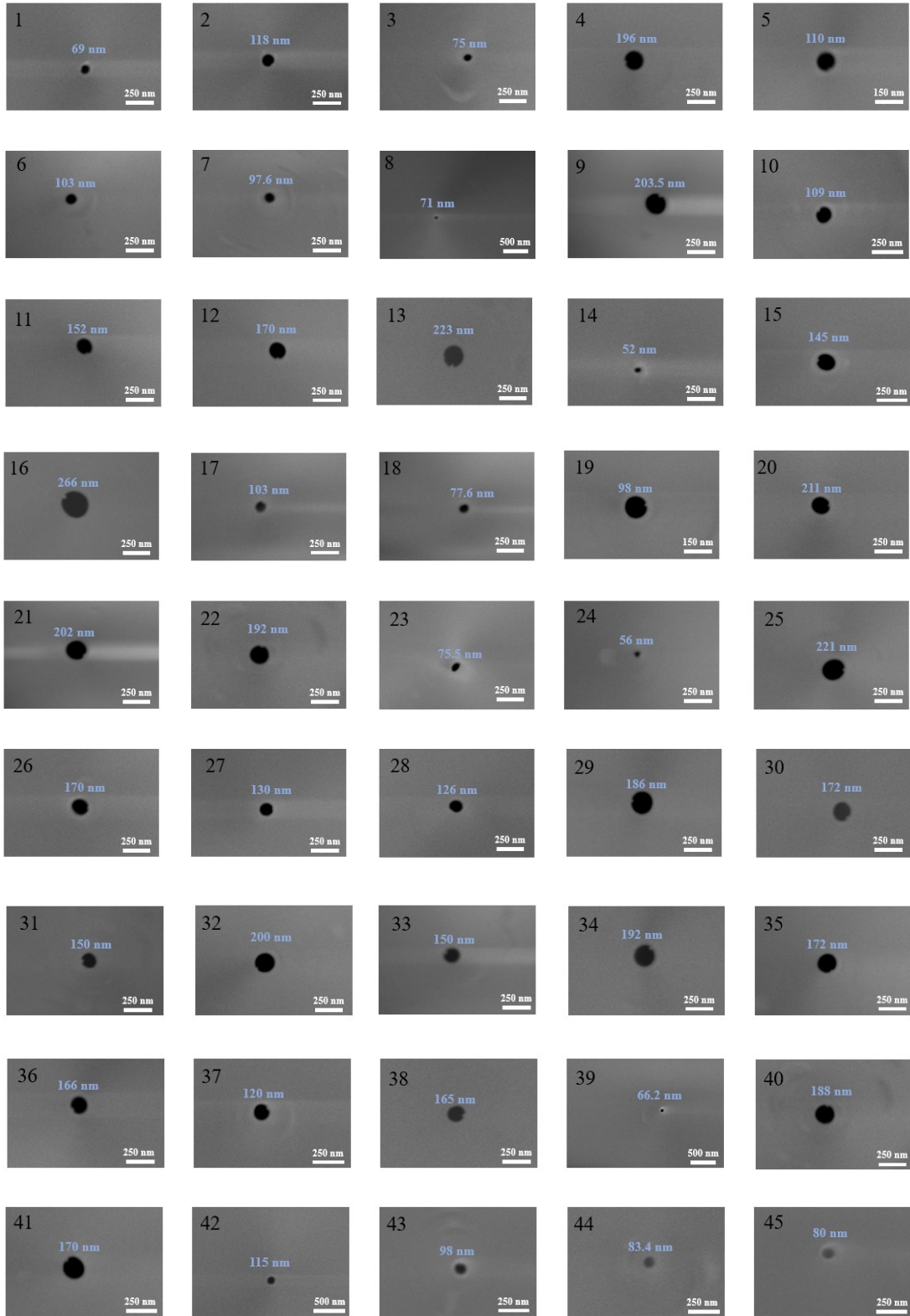
^c Haihe Laboratory for Low-dimensional Electronic Materials, Add 1 to No. 57, Wujiayao Street, Hexi District, Tianjin, 30074, P.R. China.

^d School of Precision Instrument and Opto-electronics Engineering, Tianjin University, Tianjin 300072, P.R. China

^e School of Chemistry and Chemical Engineering, Shihezi University, 832003, P.R. China

Corresponding author:

Yanqing Ma, mayanqing@tju.edu.cn, Lei Ma, lei.ma@tju.edu.cn



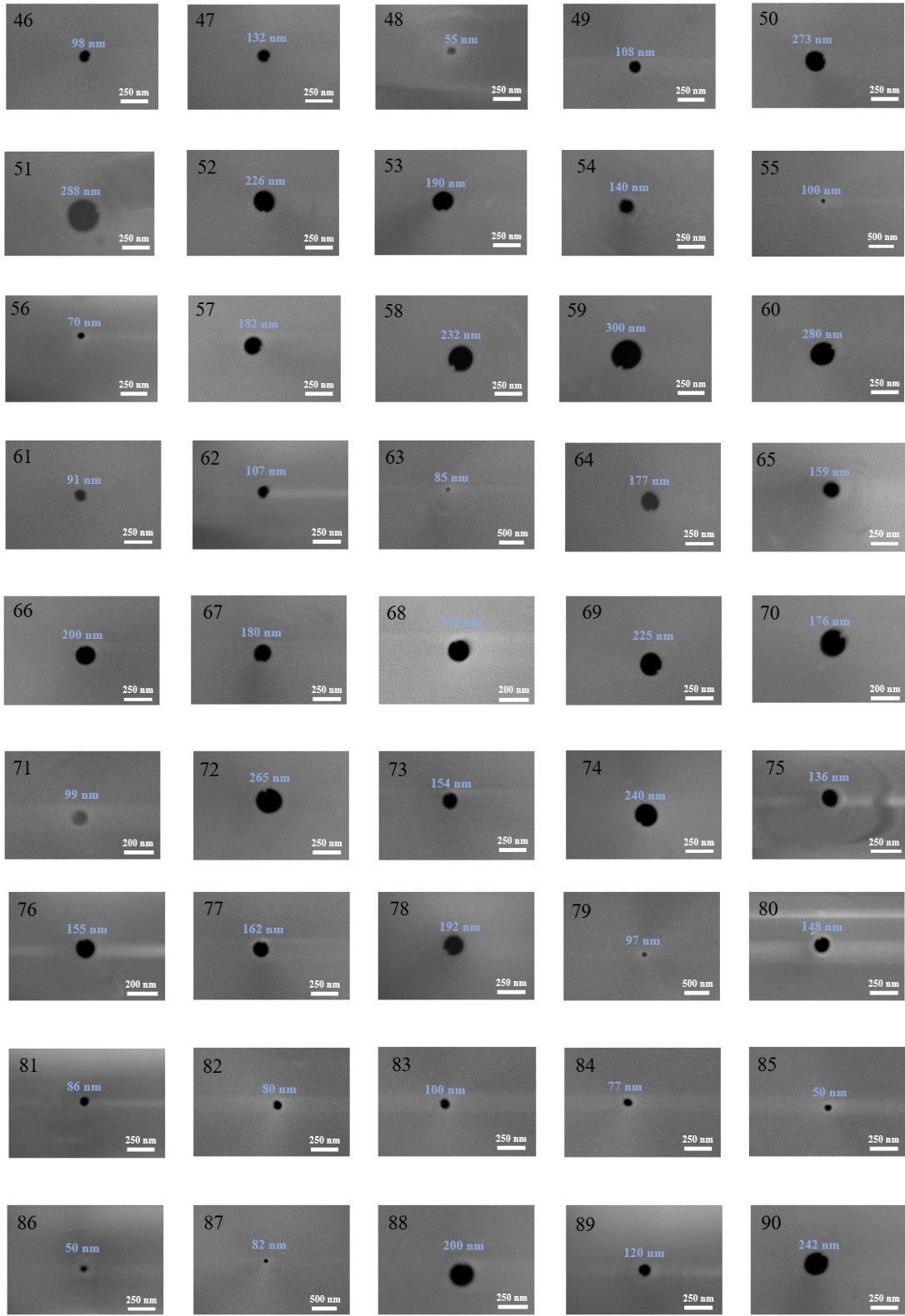




Figure S1 SEM morphology images (cross-section) of the 135 Nanopipettes samples used for training the ANN model. The numbers in each figure correspond to the serial numbers in Table S1.

Table S1 the 135 sets of Nanopipettes parameters for training the ANN model.

	HEAT	Fil	Vel	Del	Pull	Diameter
1	320	3	35	230	140	69
2	300	3	40	240	130	118
3	300	3	40	220	150	75
4	300	3	30	220	130	196
5	300	3	30	220	150	110
6	300	3	30	240	150	103
7	300	3	40	220	130	97.6
8	300	3	40	240	150	71
9	300	3	30	240	135	203.5
10	280	3	35	250	140	109
11	280	3	35	230	120	152
12	280	3	29	230	140	170
13	300	3	30	240	130	223
14	280	3	45	230	140	52
15	270	3	35	235	135	145
16	260	3	33	240	135	266
17	280	3	35	210	140	103
18	280	3	35	230	160	77.6
19	280	3	35	230	140	98
20	260	3	35	230	130	211
21	260	3	30	240	135	202
22	260	3	30	240	150	192
23	260	3	40	220	130	75.5
24	260	3	40	220	150	56
25	260	3	30	220	135	221
26	260	3	40	240	130	170
27	260	3	30	220	150	130
28	260	3	40	240	150	126
29	250	3	35	230	135	186
30	260	3	38	240	135	172
31	260	3	40	240	135	150
32	250	3	35	235	135	200
33	290	3	35	235	110	150
34	255	3	35	235	120	192
35	255	3	35	235	130	172
36	260	3	35	235	130	166
37	290	3	35	235	130	120
38	250	3	35	220	135	165
39	300	4	38	220	150	66.2
40	255	3	35	235	135	188
41	260	3	35	235	135	170
42	280	3	35	235	135	115

Table S1 (Continued)

43	290	3	35	235	135	98
44	320	3	35	235	135	83.4
45	310	3	35	235	135	80
46	300	3	35	235	135	98
47	255	3	35	235	150	132
48	320	3	35	235	150	55
49	255	3	35	235	160	108
50	230	1	38	240	120	273
51	240	3	35	240	130	288
52	250	3	35	240	130	226
53	260	3	35	240	130	190
54	280	3	35	240	130	140
55	300	3	35	240	130	100
56	310	3	35	240	130	70
57	260	3	35	240	135	182
58	250	3	35	240	135	232
59	240	3	35	240	135	300
60	245	3	35	240	135	280
61	270	3	35	240	140	91
62	280	3	35	240	140	107
63	300	3	35	240	140	85
64	250	3	35	240	140	177
65	260	3	35	240	140	159
66	240	3	35	240	140	200
67	265	3	35	245	130	180
68	280	3	35	245	130	150
69	250	3	35	245	135	225
70	270	3	35	245	135	176
71	300	3	35	245	140	99
72	250	3	35	250	135	265
73	280	3	35	250	135	154
74	240	3	35	230	140	240
75	300	4	35	220	135	136
76	280	4	35	220	135	155
77	320	4	35	235	130	162
78	290	4	35	235	140	192
79	300	4	35	235	140	97
80	270	4	35	235	150	148
81	280	4	35	235	150	86
82	290	4	35	235	150	80
83	300	4	35	235	150	100
84	310	4	35	235	150	77
85	320	4	35	235	150	50

Table S1 (Continued)

86	325	4	35	235	150	50
87	290	4	35	240	150	82
88	300	4	35	250	150	200
89	320	4	35	250	150	120
90	240	2	35	235	135	242
91	245	2	35	235	135	202
92	255	2	35	235	135	182
93	270	2	35	235	135	121
94	270	3	35	240	120	164
95	245	2	35	240	130	230
96	240	2	35	240	135	292
97	310	2	35	230	140	71
98	270	2	35	230	140	115
99	270	2	35	240	150	82
100	270	2	35	245	130	168
101	300	2	35	245	130	91
102	250	2	35	245	130	268
103	240	2	35	245	130	317
104	250	2	35	240	150	160
105	270	2	35	240	120	188
106	230	2	35	240	150	306
107	250	2	35	240	135	210
108	240	2	35	242	135	276
109	300	1	35	240	135	94
110	270	1	35	240	135	125
111	260	2	38	220	130	96
112	300	2	32	240	150	111
113	270	2	35	230	120	148
114	250	2	32	240	130	261
115	260	2	32	220	150	121
116	260	2	32	220	130	206
117	260	2	32	240	150	145
118	260	2	38	240	140	115
119	260	2	38	240	130	135
120	260	2	38	240	150	88.8
121	300	2	32	220	130	104
122	300	2	32	240	130	142
123	300	2	38	220	130	75
124	300	2	38	220	150	70
125	300	2	38	240	130	101
126	300	2	38	240	150	76
127	230	1	35	240	135	320
128	230	1	35	240	150	260

Table S1 (Continued)

129	235	1	35	240	135	303
130	240	1	35	230	130	191
131	240	1	35	240	135	275
132	250	1	35	240	120	243
133	250	1	35	240	135	188
134	250	1	35	240	150	136
135	250	1	40	240	120	184

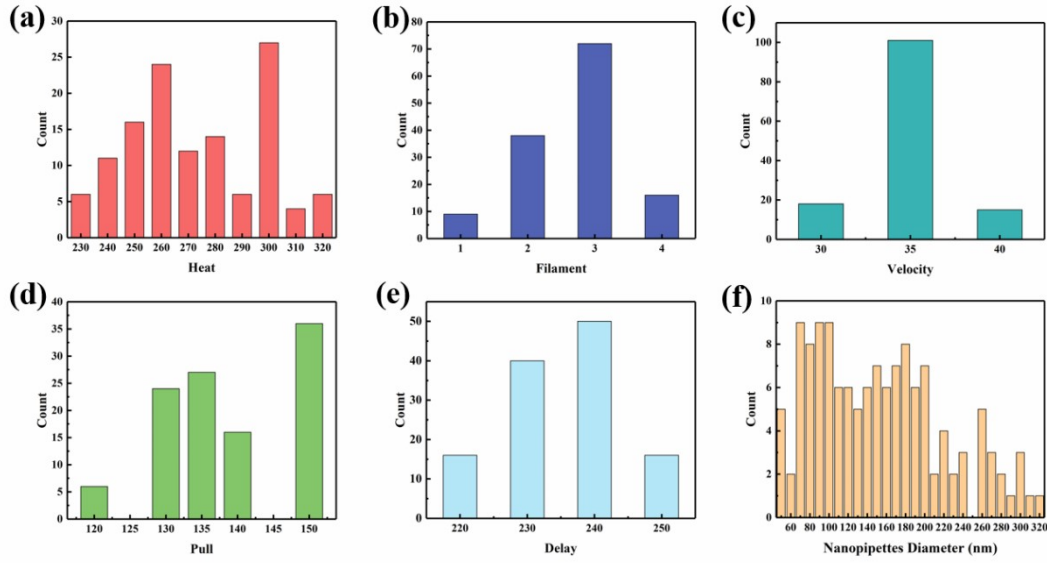


Figure S2 Frequency distributions of the key fabrication parameters and resulting nanopipette diameters. (a) Heat; (b) Filament; (c) Velocity; (d) Pull; (e) Delay; (f) Nanopipette diameter (nm).

As shown in Figure S2, it should be noted that the fabrication parameters appear to be concentrated in the middle regions, with fewer data points near the parameter boundaries. This is not due to an uneven experimental design, but arises from the instability of the pulling process near the parameter limits: when parameters approach the edges of the feasible range, the nanopipette aperture often exhibits an abrupt change (similar to Point 4 in Figure 4b), yielding invalid or unusable samples. These unstable and meaningless data were excluded during preprocessing, leaving only valid and reproducible data within the reliable parameter range. Notably, even though the fabrication parameters are concentrated in the middle range, the corresponding nanopipette aperture values are evenly distributed across the target range of 50–1000 nm, which ensures that the dataset is representative and sufficient for model training and prediction within the practical application scope.

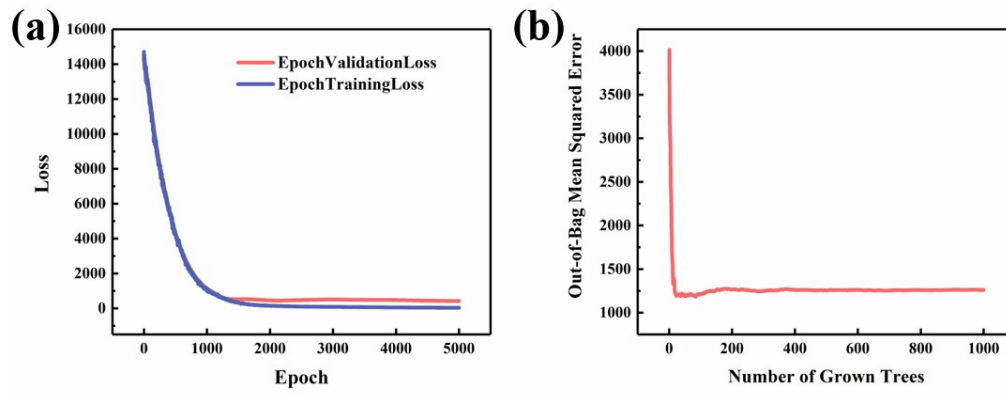


Figure S3 (a) Convergence curves of training and validation loss for the ANN over 5000 iterations; (b) Evolution of the out-of-bag mean squared error (OOB-MSE) as a function of the number of decision trees in the random forest model.

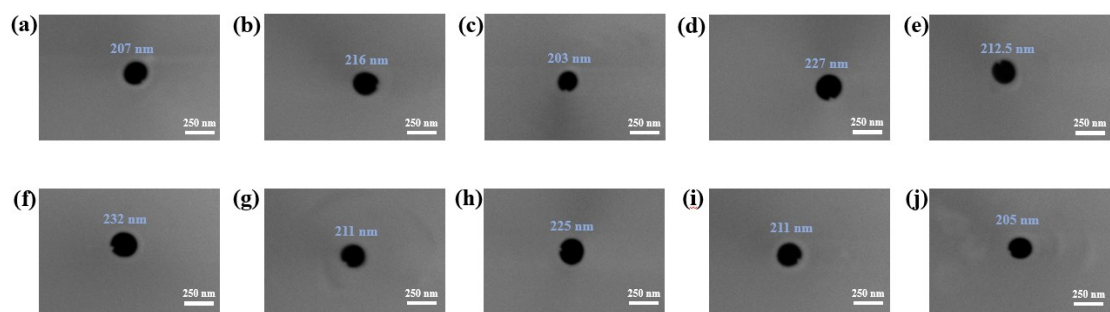


Figure S4 (a-j) SEM cross-sectional images of ten nanopipette tips fabricated under the same parameter set (Heat 250, Filament 3, Velocity 35, Delay 235, Pull 135).

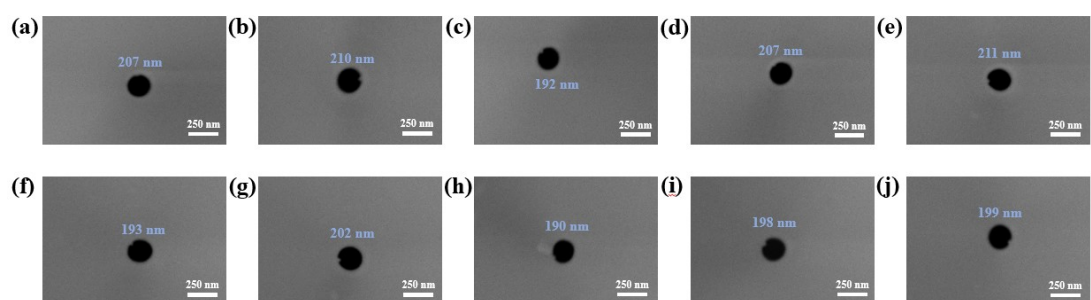


Figure S5 (a-j) SEM cross-sectional images of ten nanopipette tips fabricated under the same parameter set (Heat 252, Filament 3, Velocity 35, Delay 235, Pull 135).

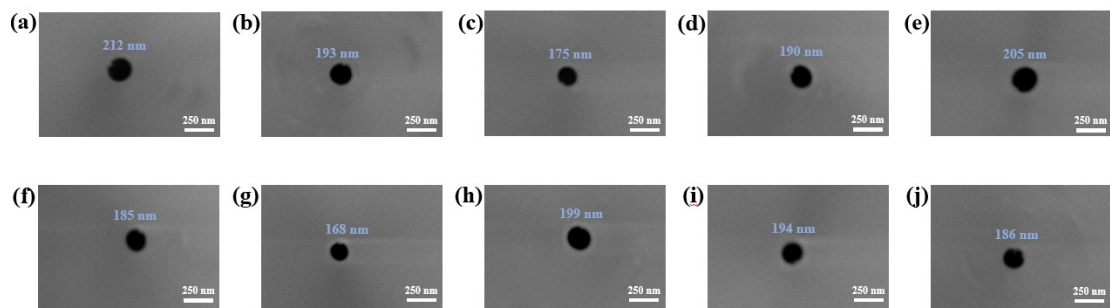


Figure S6 (a-j) SEM cross-sectional images of ten nanopipette tips fabricated under the same parameter set (Heat 255, Filament 3, Velocity 35, Delay 235, Pull 135).

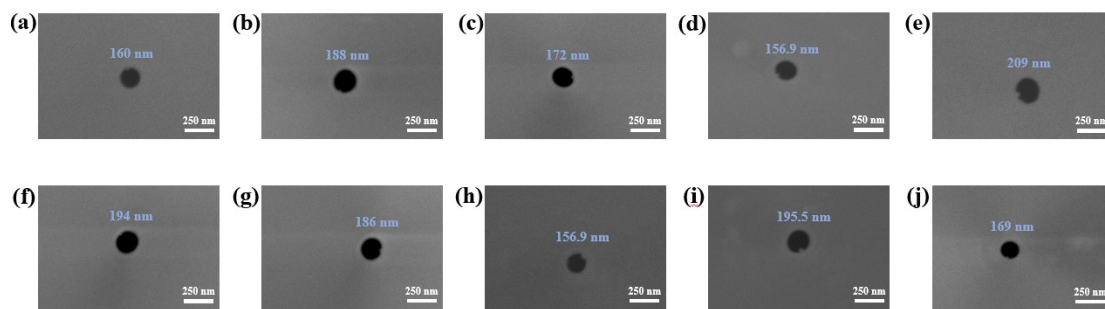


Figure S7 (a-j) SEM cross-sectional images of ten nanopipette tips fabricated under the same parameter set (Heat 252, Filament 3, Velocity 35, Delay 235, Pull 137).

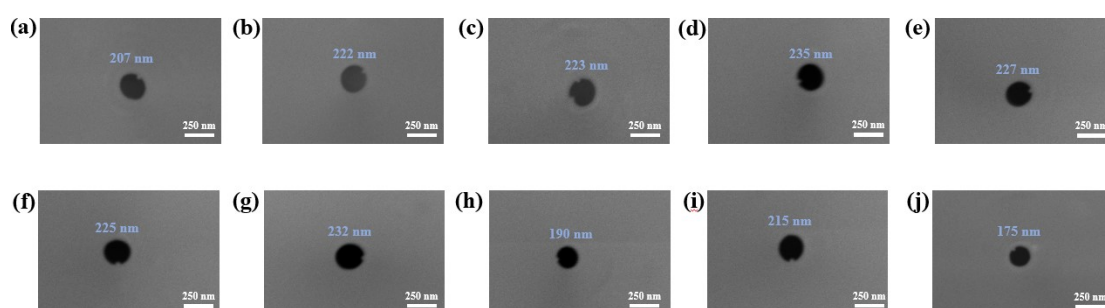


Figure S8 (a-j) SEM cross-sectional images of ten nanopipette tips fabricated under the same parameter set (Heat 252, Filament 3, Velocity 35, Delay 235, Pull 133).

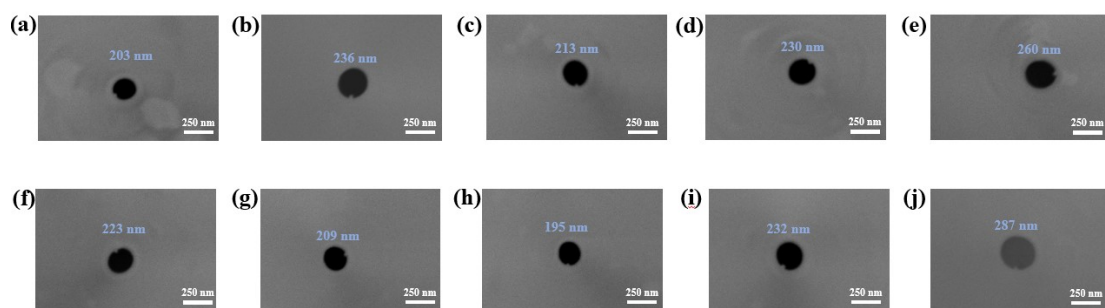


Figure S9 (a-j) SEM cross-sectional images of ten nanopipette tips fabricated under the same parameter set (Heat 252, Filament 3, Velocity 35, Delay 237, Pull 135).

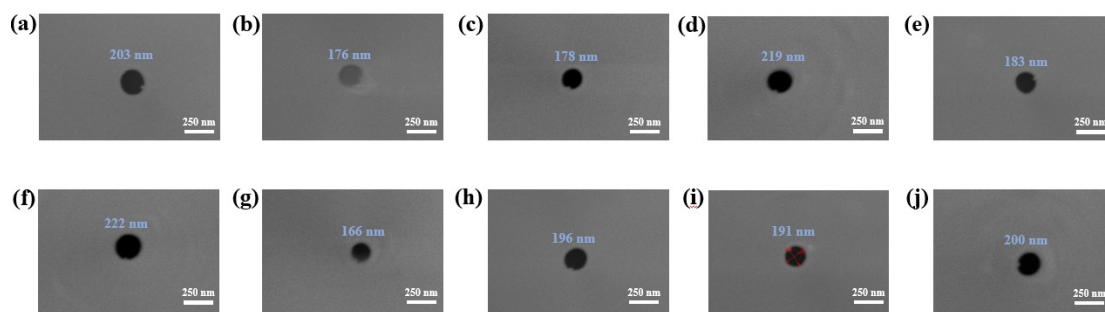


Figure S10 (a-j) SEM cross-sectional images of ten nanopipette tips fabricated under the same parameter set (Heat 252, Filament 3, Velocity 35, Delay 233, Pull 135).

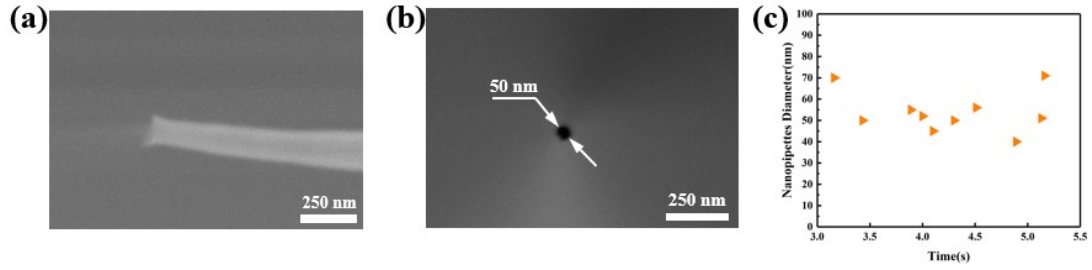


Figure S11 SEM characterization of a 50 nm nanopipette fabricated with parameters Heat 320, Filament 4, Velocity 35, Delay 235, Pull 150. (a) Top-down view. (b) Cross-sectional view. (c) Diameter measurements from ten independent fabrication runs.

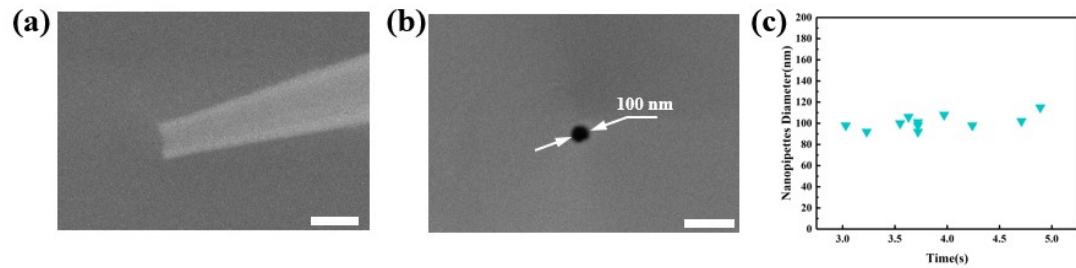


Figure S12 SEM characterization of a 100 nm nanopipette fabricated with parameters Heat 300, Filament 4, Velocity 35, Delay 235, Pull 145. (a) Top-down view. (b) Cross-sectional view. (c) Diameter measurements from ten independent fabrication runs.

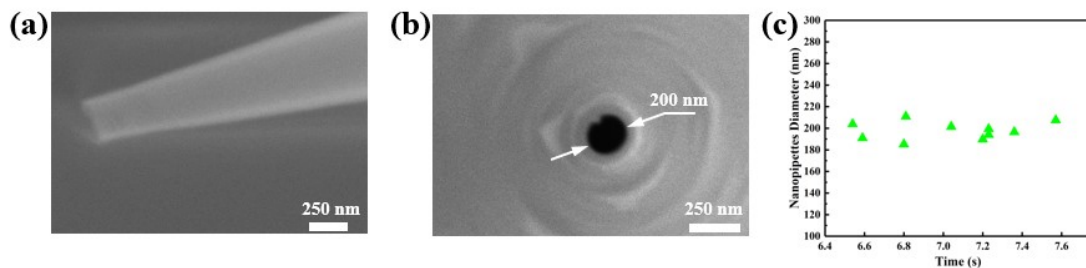


Figure S13 SEM characterization of a 200 nm nanopipette fabricated with parameters Heat 252, Filament 3, Velocity 35, Delay 235, Pull 135. (a) Top-down view. (b) Cross-sectional view. (c) Diameter measurements from ten independent fabrication runs.

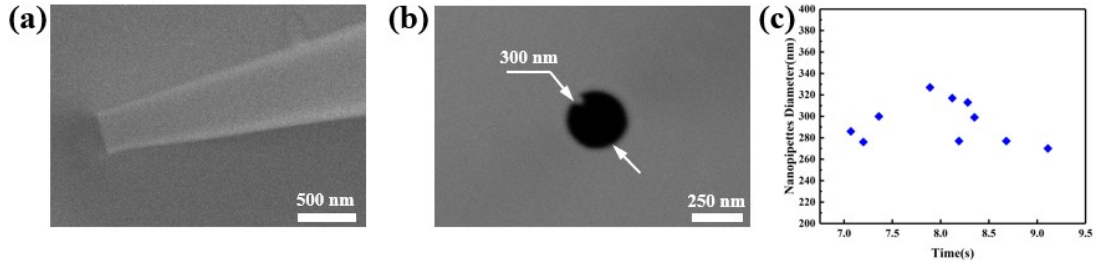


Figure S14 SEM characterization of a 300 nm nanopipette fabricated with parameters Heat 240 Filament 2, Velocity 35, Delay 240, Pull 135. (a) Top-down view. (b) Cross-sectional view. (c) Diameter measurements from ten independent fabrication runs.

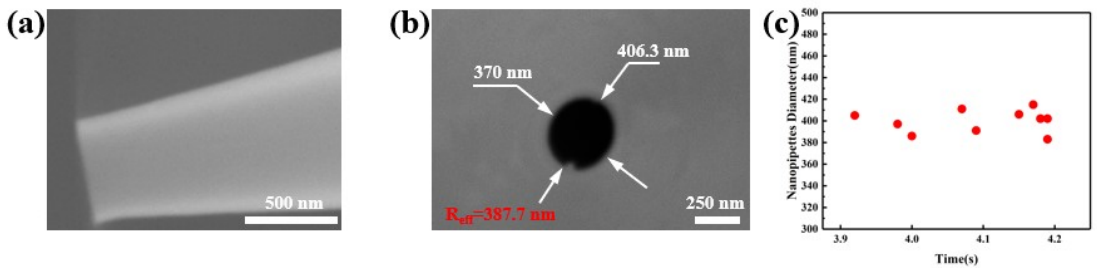


Figure S15 SEM characterization of a 400 nm nanopipette fabricated using a two-line program: Heat 300, Filament 3, Velocity 40, Delay 255, Pull 0 /Heat 300, Filament 3, Velocity 70, Delay 128, Pull 35. (a) Top-down view. (b) Cross-sectional view.

Equivalent circular radius is calculated as $R_{eff} = \sqrt{a \times b}$. (c) Diameter distribution from ten independent fabrication runs.

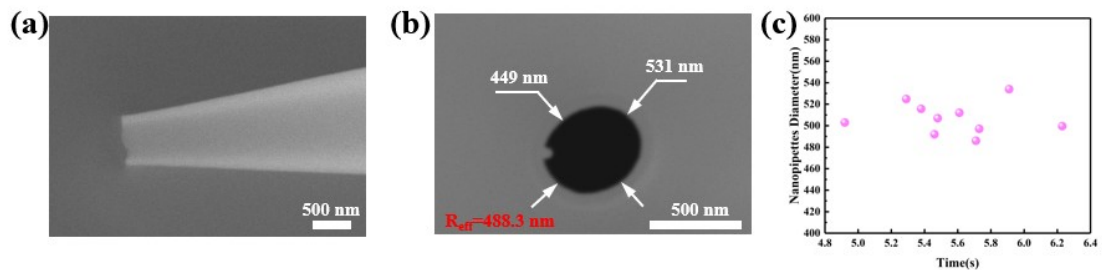


Figure S16 SEM characterization of a 500 nm nanopipette fabricated using a two-line program: Heat 270, Filament 3, Velocity 40, Delay 255, Pull 0 /Heat 270, Filament 3, Velocity 70, Delay 128, Pull 35. (a) Top-down view. (b) Cross-sectional view.

Equivalent circular radius is calculated as $R_{eff} = \sqrt{a \times b}$. (c) Diameter distribution

from ten independent fabrication runs.

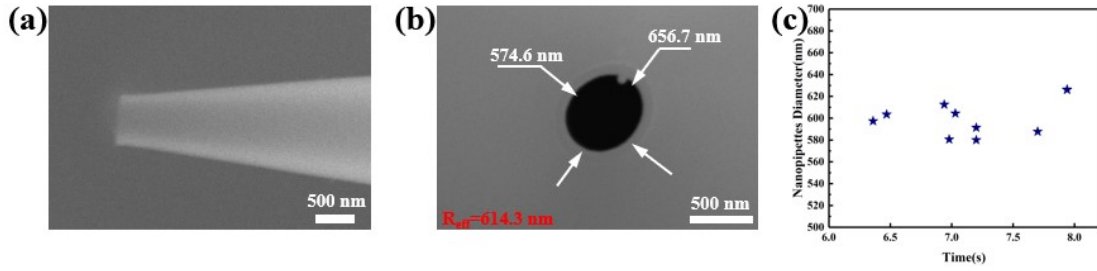


Figure S17 SEM characterization of a 600 nm nanopipette fabricated using a two-line program: Heat 260, Filament 3, Velocity 40, Delay 255, Pull 0 /Heat 260, Filament 3, Velocity 70, Delay 128, Pull 35. (a) Top-down view. (b) Cross-sectional view.

Equivalent circular radius is calculated as $R_{eff} = \sqrt{a \times b}$. (c) Diameter distribution from ten independent fabrication runs.

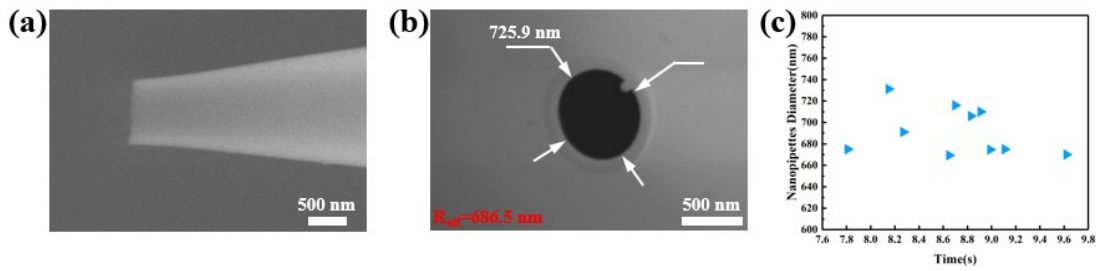


Figure S18 SEM characterization of a 700 nm nanopipette fabricated using a two-line program: Heat 245, Filament 3, Velocity 40, Delay 255, Pull 0 /Heat 245, Filament 3, Velocity 70, Delay 128, Pull 35. (a) Top-down view. (b) Cross-sectional view.

Equivalent circular radius is calculated as $R_{eff} = \sqrt{a \times b}$. (c) Diameter distribution from ten independent fabrication runs.

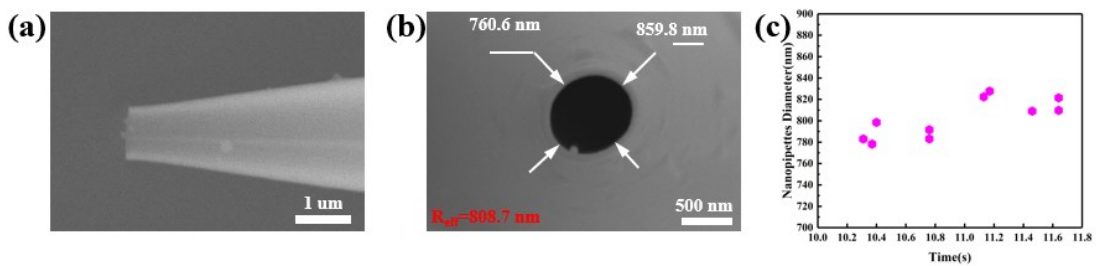


Figure S19 SEM characterization of a 800 nm nanopipette fabricated using a two-line program: Heat 240, Filament 3, Velocity 40, Delay 255, Pull 0 /Heat 240, Filament 3,

Velocity 70, Delay 128, Pull 35. (a) Top-down view. (b) Cross-sectional view. Equivalent circular radius is calculated as $R_{eff} = \sqrt{a \times b}$. (c) Diameter distribution from ten independent fabrication runs.

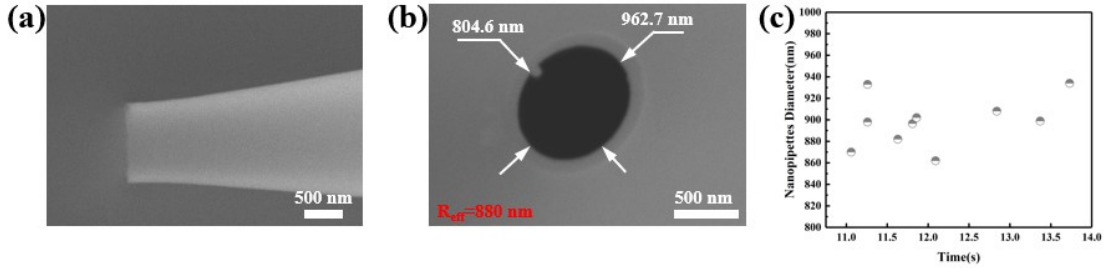


Figure S20 SEM characterization of a 900 nm nanopipette fabricated using a two-line program: Heat 230, Filament 3, Velocity 40, Delay 255, Pull 0 /Heat 230, Filament 3, Velocity 70, Delay 128, Pull 35. (a) Top-down view. (b) Cross-sectional view.

Equivalent circular radius is calculated as $R_{eff} = \sqrt{a \times b}$. (c) Diameter distribution from ten independent fabrication runs.

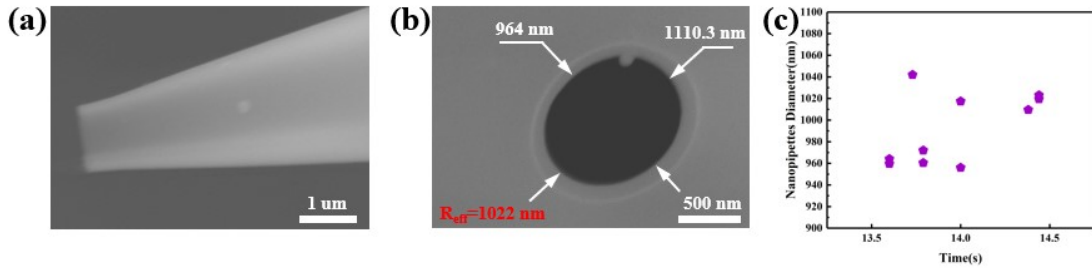


Figure S21 SEM characterization of a 1000 nm nanopipette fabricated using a two-line program: Heat 227, Filament 3, Velocity 40, Delay 255, Pull 0 /Heat 227, Filament 3, Velocity 70, Delay 128, Pull 35. (a) Top-down view. (b) Cross-sectional view. Equivalent circular radius is calculated as $R_{eff} = \sqrt{a \times b}$. (c) Diameter distribution from ten independent fabrication runs.

Table S2 Pulling parameters for 50 nm-1000 nm nanopipettes

						Nanopipettes
	Heat	Filament	Velocity	Delay	Pull	Diameter(nm)
1	320	4	35	235	150	50
2	300	4	35	235	145	100
3	252	3	35	235	135	200
4	240	2	35	240	135	300
5	300	3	40	255		
	300	3	70	128	35	400
6	270	3	40	255		
	270	3	70	128	35	500
7	255	3	40	255		
	255	3	70	128	35	600
8	245	3	40	255		
	245	3	70	128	35	700
9	240	3	40	255		
	240	3	70	128	35	800
10	230	3	40	255		
	230	3	70	128	35	900
11	227	3	40	255		
	227	3	70	128	35	1000
	240	3	70	128	35	800
10	230	3	40	255		
	230	3	70	128	35	900
11	227	3	40	255		
	227	3	70	128	35	1000